Fabrication and testing of a microfluidic device for multi-cell analysis of mechanical properties of cells

Wijnands, S.F.L.

Award date:
2013

Fabrication and testing of a microfluidic device for multi-cell analysis of mechanical properties of cells

S.F.L. Wijnands

Master thesis

Master Thesis

Eindhoven University of Technology
Department of Mechanical Engineering
Computational and Experimental Mechanics

Prof. dr. ir. J. M. J. den Toonder
Dr. H. M. Wyss
A. Ravetto Msc
Eindhoven, May 2, 2013

Summary

The need for medical care will grow in western society in the coming years due to the proportional increase of the ageing population and an unhealty lifestyle. Cardiovascular diseases and cancer are responsible for the deaths of many people each year. When these diseases are diagnosed in an early stage the changes of survival greatly improves. However the procedures used to diagnose these kind of diseases are very time consuming and expensive.

A method to screen for diseased cells is by detecting changes in mechanical behaviour between healty and diseased cells. Several techniques have been established to test single cell behavior, however most of these techniques can only test a single cell at a time, making them very time-consuming. For this reason a cheap device is designed in which a cell can be trapped and deformed. By chaining together segments multiple cells can be trapped simultaneously. By measuring the deformation of the cells at different flow rates mechanical properties such as cortical tension can be determined. At a certain critical flow rate the cells are squeezed out of their traps, which is also used to characterize their behavior.

Soft lithography is used to create a master wafer, which in turn is used to create a PDMS device for the analysis of cells. Using this device HL-60 cells were analysed. Analysis shows there is a certain pressure at which multiple cells squeeze trough their traps . This critical pressure range might be used as a mechanical property indicator. Unfortunately, due to leaking accurate values could not be determined. The cortical tension, calculated using the liquid drop model, has been determined to be five to ten times higher than typical values reported in literature, which can also be explained by time depended properties of the cells and the leakage. The thesis will conclude with a list of suggestions for future designs, to improve the effectiveness of the device.

Contents

Introduction

Any individual needs, at some point in his or her life, medical care. Heart diseases, HIV/aids and cancer are responsible for the deaths of many people each year[1]. Many of these diseases benefit from an early discovery to improve the chances of survival. Unfortunately diagnosis for these kind of diseases, for example cancer, are still time-consuming, expensive, and may not be entirely without risk, using techniques such as X-ray imaging[2]. In addition, for many people the advanced medical equipment is simply not accessible, as is the case in most developing countries. Techniques to quickly screen for this disease could thus save many lives. A method to detect a cancer or diseased cell is by using blood tests. A blood test will search for certain antigens in the blood, produced by the presence of the diseased cells[2]. However they are usually specific and therefore diagnosing a person for multiple diseases can be very time-consuming, requiring many rounds looking for different antigens, just to screen for the most common diseases.

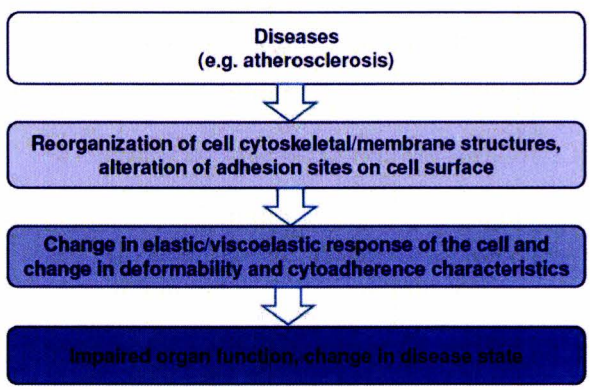

Figure 1: Pathways between cellular structure-properties and diseased state of cells[4]

There may be another way to screen for diseased cells, as diseased cells may have undergone changes in the cytoskeleton reorganization and membrane structures, which in turn can affect mechanical deformability and elastic modulus, as illustrated in figure 1. These changes in mechanical properties of cells may be used as an indicator for the presence of diseased cells.

Over the course of the last few years several techniques have been developed to study and quantify the mechanical properties of cells at the single cell level. Examples of these existing techniques are optical tweezers, micropipette aspiration, atomic force microscopy and several microfluidic techniques. We will first discuss these existing techniques, after which we will explain our new approach, which has several important advantages over the current approaches.

Existing techniques

Optical tweezers

Optical tweezers can manipulate nanometer- and micron-sized particles by using a highly focused laser beam[5 3]. The beam is usually focused by a microscope objective. The beam waist (where the beam is narrowest) exhibits a strong electromagnetic field gradient. This gradient can be used to attract dielectric particles towards the center of the beam, where the field is strongest. However, the actual trapping point of the particle is slightly further along the direction of beam propagation; this is due to the conservation of momentum. Photons from the laser that are absorbed or scattered by the dielectric particle impart momentum to this particle, resulting in a minor displacement.

In order to determine the properties of a cell, two dielectric particles are attached to opposite sides on the surface of the cell, this is shown schematically in figure 2 . One is kept in a steady position, for instance by attaching it to a glass slide, while the other particle is trapped by the laser. In some cases it is also possible to connect the cell itself to a glass side, in which case only one dielectric particle is needed. When moving the particle trapped by the laser, the particle will exert a force on the cell, which is used to measure the response. The distance between the center of the beam and center of the dielectric particle determines the force that is being applied. For small distances, this relationship is linear and the principle is analogous to a spring following Hooke's law; force equals stiffness times distance. The force exerted is usually between a couple a pN to hundreds of pN. Some disadvantages of this technique are the low force that can be applied, the need of surface treatment to enhance the attachment of the dielectric beads, the time consuming activity of aligning the laser and mirrors and finally the expensive equipment usage such as the laser and several mirrors.

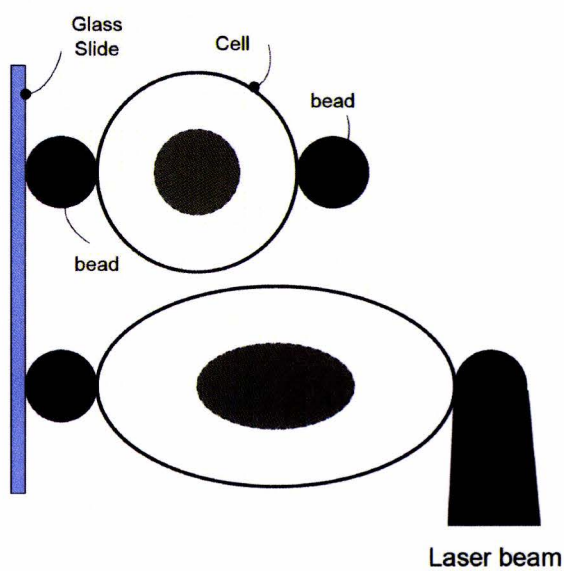

Figure 2: Optical tweezers, the upper image shows two dielectric beads are placed on opposite sites of a bead. One of these beads is moved using a laser beam in the lower image[3]

Micropipette aspiration

Micropipette aspiration uses a glass micropipette to suck in a part of the cell by applying a negative pressure[3], this is shown in figure 3. The inner diameter of the pipette is chosen sufficiently small, such that there will be enough deformation of the cell when the negative pressure is increased in a stepwise manner, but large enough to be able to suck in the cell as a whole. This technique uses existing models for the relationship between the suction pressure, the pipette tip diameter, cell size and length of the cell in the pipette, to measure for example the stiffness and the cortical tension.

The test setup for a basic micropipette aspiration experiment consists of a pressure regulator, a micropipette positioning system and a microscope, equipped with a camera. The experiment itself is relatively straightforward. The pipette is installed, with the tip aligned with the focal plane of the microscope. Selected cells are aligned with the tip, then aspired using a negative pressure while the microscope with camera records the observations for later analysis. Despite the simplicity of the tools, the process consists of delicate procedures, and the experimentation time severely depends on the skill of the researcher. The used pressures are typically small (less than 100 Pa), which means that the system can be disturbed by fluctuations in temperature or humidity as well as mechanical vibrations.

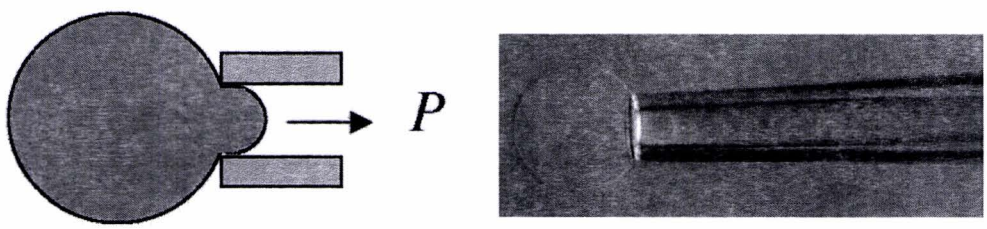

Figure 3: The left image shows a schematic representation of micropipette aspiration, the right image shows a real life application[6 7]

In a recent modification of this technique, termed Capillary Micromechanics[8], the process is actually reversed. A cell is pushed into the pipette by applying a low pressure until it gets stuck, as the diameter of the pipette towards the tip is slowly decreasing. A stepwise pressure increase is then used to push the cell to the tip and acquire information about the cell by measuring the volume and shape change. An advantage of this method is that the cell and the pipette tip are automatically aligned. Moreover, Capillary Micromechanics also enables characterizing both the compressive and the shear elastic modulus in a single experiment. The measured moduli should also better reflect the mechanical properties of the entire cell, rather than the local properties, for example those of the cell wall. However, both methods can only characterize a single cell at a time, making it time-consuming to characterize a cell type, as properties differ from cell to cell and many experiments are needed to determine the average mechanical properties.

Atomic force microscopy

Atomic force microscopy (AFM) relies on the detection of forces between the AFM tip and a surface[9]. The tip, usually a sharp probe, is attached to a flexible cantilever. The tip is brought in contact with the surface, over which it will move in a lateral direction. The deflection of the cantilever, which is in most cases measured with a laser beam, is an indication of the topography of a surface. For cell properties research, the probe tip is actually used to apply pressure on the surface of a cell instead of following its surface. The tip is placed on the surface of a cell, however it does not move in a lateral direction along the surface, but in a perpendicular direction. When the tip is away from the surface, there is no deflection and hence the force is zero. When the tip is lowered and it touches the surface, the stiffness of the cell will determine the amount of force applied to the cantilever, resulting in a deflection which is measured by a laser, this is shown in figure 4 . An obvious disadvantage of this method is the use of expensive equipment. It is also only capable of analysing a single cell at a time, and requires a surface to press the cell against. This makes it hard to measure cells in a medium. Finally only a local measurement is performed, making the results dependent on the position of the probe in relation to the cell.

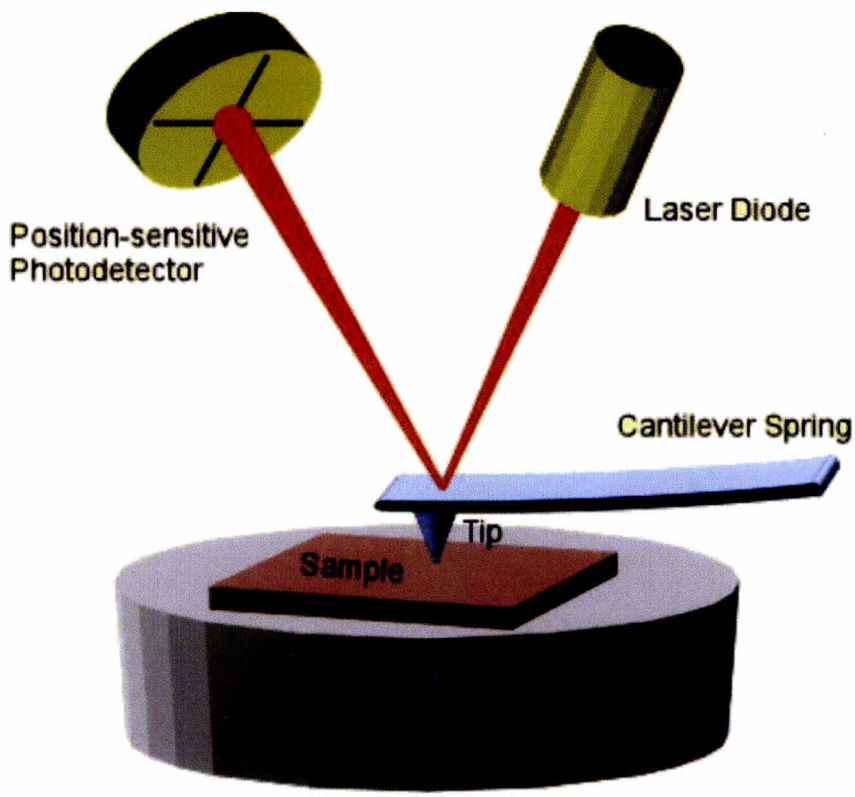

Figure 4: The working principle of atomic force microscopy[10]

Microfluidic techniques

Improvements in micro fabrication technologies allow microstructures to be used for various applications over the recent years[3]. The devices, generally created using soft lithography, are cost-efficient, disposable, and relatively easy to produce. For cell properties research, the devices can be organized into two categories: Microstructures that mechanically deform the cell by forming an obstacle and microstructures that use flow to stretch cells. The first category consists of a single long channel, in which a cell is deformed, be it by introducing a gradual tightening of the channel, as is shown in figure 5A , or by a sudden but constant contraction, as is shown in figure 5B, 5C and 5D . Using these devices parameters such as geometrical changes and transit time are observed. These can be used to find differences, and therefore distinguish, between healthy and diseased states. The second category relies on converging streamlines, with the cell located in the centre, to cause cell deformation. Hyperbolic- and crossroad shaped structures are used to create these streamlines, see figure 5E and 5F . By analysing the ratio of the length of both axes of a cross-sectional area of a cell the deformability of the cell can be quantified.

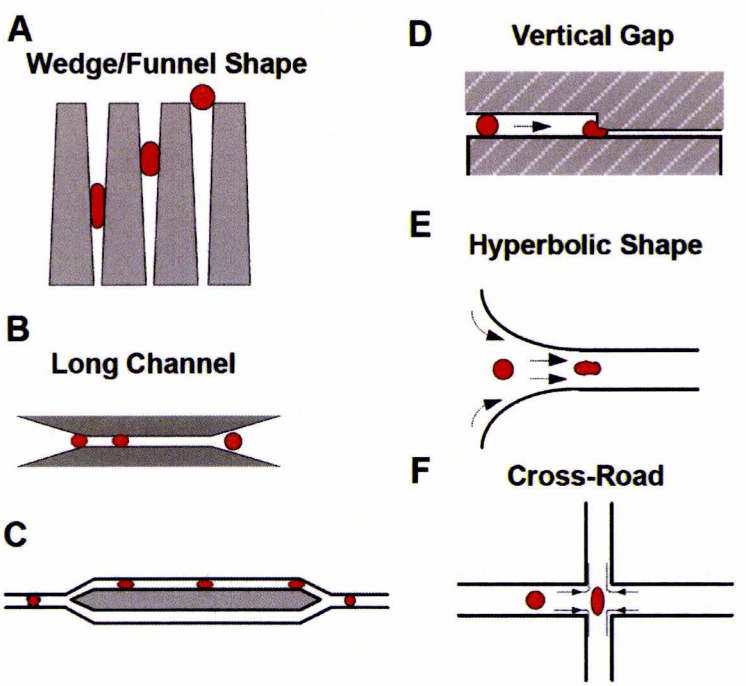

Figure 5: Schematic illustrations of various micro-scale constructions to cause deformation of single suspended cells either through direct contact of cells with obstacles (A-D) or via converging streamlines where the cells are in the center of the flows (E,F) [10]

Using a microfluidic technique has distinct advantages over traditional methods. Since the cell and the structure are on the same focal plane, it is much easier to maintain focus over the course of an experiment. Costs are drastically reduced as almost no expensive equipment needs to be used. Furthermore, as the cost of a PDMS device is low, a device can easily be replaced in case of damage or blockage of the channels by, for example, debris or dust. A disadvantage is that in most cases, as was with micropipette aspiration, a camera is required in combination with a microscope to track the deformation of the cell.

New approach

In this report we introduce a new approach which combines the advantages of using microfluidic techniques with those using a micropipette, while shortening the long experimentation time, as this was a main disadvantage of the previously mentioned techniques. This will be improved by doing multiple experiments in parallel. The goal of this thesis is therefore to design a simple to use and cost-efficient device capable of measuring the mechanical properties of multiple cells simultaneously.

The steps taken to produce the microfluidic device, consisting of multiple single cell traps in series, will be described. In the design, a constant flow rate is generated which creates well-controlled pressure gradients that mechanically deform the cells caught in the traps. Clogging of the device is prevented by introducing a bypass channel. This design is turned into a mask and soft lithography is used for the production of actual polydimethylsiloxane (PDMS) devices. After using an initial design to test the approach, the final design has been tested with HL-60 leukemia cells. At the end of this thesis the results will be discussed, and possible improvements will be suggested.

Chapter 1

Device concept and design

1.1 Main principle

To measure the deformability of a cell, our concept combines the principle of micropipette experiments with a microfluidic device. The cell is trapped in a narrowing channel, and then subjected to a change in the pressure drop over the cell. This is done for dozens of cells simultaneously, which is accomplished by chaining together identical segments.

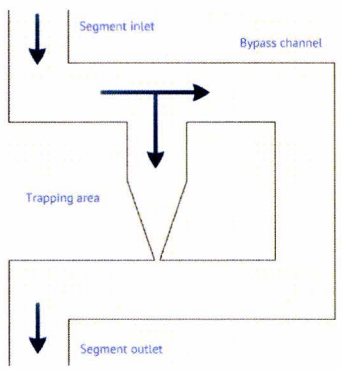

(a) A segment of the newly designed device. A segment consists of an inlet and an outlet, as well as trapping area and a bypass channel

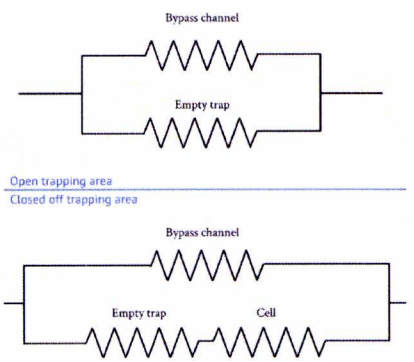

(b) A schematic representation of the resistances in a segment when there is no cell trapped (upper image) and when there is a cell/particle trapped (lower image). In the upper case $R_bypass > R_empty$ trap, in the lower case $R_bypass < R_emptytrap + R_cell$, as the cell blocks an area of the trapping area increasing its total hydraulic resistance [11]

Figure 1.1

A segment of the device consists of two main parts: a trapping area and a bypass channel as show schematically in figure 1.1a . These segments can be repeated consecutively to increase the number of cells that can be analysed. The bypass channel is a regular square channel while the trapping area contains a converging channel with a certain tip diameter, much like a microcapillary. During an experiment a cell solution is flown in from the top. Because of the small dimensions in microfluidic devices this flow is laminar, causing the path a cell takes to be dependent only on the hydraulic resistance difference between the trapping area and the bypass channel. This hydraulic resistance is caused by the viscous dissipation of mechanical energy by internal friction and will be explained in the next section. When a cell, which has approximately the size of the channel width, approaches the segment, it can either flow through the trapping area or through the bypass channel. The length of the bypass channels is chosen as such, that their resistance is initially higher than the resistance of the trap. This means that most of the liquid flow, at least more than 50%, will pass through the trapping area, taking the cell with it. The cell diameter is larger than the trap diameter, causing it to remain in the trapping area as long as it does not mechanically deform.

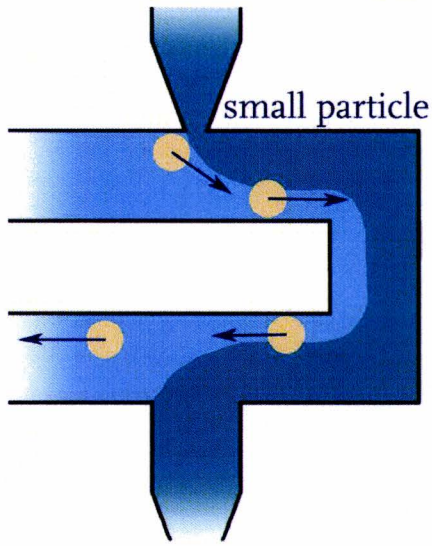

Figure 1.2: This figure shows the path a smaller cell could take, causing it not to get trapped [11]

Once trapped, the cell will block most of the flow through the trapping area, which will increase the total resistance of this area, increasing it beyond the resistance of the bypass channel. This is shown schematically in figure 1.1b . The next cell from the cell solution that passes will therefore flow into the bypass channel and around the previously trapped cell into the next segment.

For analysing purposes, we assume that the pressure drop over a cell in a trap is dependent only on the resistance of the bypass channel and the flow rate once a cell completely blocks the trapping area; the larger the resistance, the higher the pressure drop. Increasing the pressure drop in a stepwise manner will mechanically deform the cell, until the pressure rises enough to squeeze the cell through the trap; the geometrical changes as well as this critical pressure can then be used to compare the properties of a specific cell with a diseased one or with other kinds of cells.

The dimensions of the device should be tuned to the size of the cell to be tested. The design relies on the channel width to be approximately equal to the cell diameter. When cell diameter and channel width are the same, the position of the cell in the channel is independent from the flow lines. However, when the width of the channel is smaller than the cell diameter, whether or not the cell gets trapped is now also dependent on the flow lines, as can be seen figure 1.2. This may cause some cells to get trapped while others of identical size may just flow through the bypass channels, depending on their initial position in the channel.

A great advantage of the design is that a cell, if it did not get trapped, will simply move towards the exit channel and flow out of the device through the bypass channels without clogging the device. Therefore minor differences in cell diameter, which may vary from cell to cell, do not have a large influence as is the case for example in micropipette aspiration. Another advantage is that the pressure drop can be kept constant merely by having a constant flow rate. As the segments are placed in series the pressure drop over the trapped cells will not be affected when one trapped cell squeezes through. This will only have an effect on the pressure drop of the entire device as the total channel length will decrease.

1.2 Hydraulic resistance

The hydraulic resistance of the segments can be calculated using OhmâTMs law for fluid flow through channels:

$$R_h = \frac{\Delta P}{Q} \tag{1.1}$$

With R_h the hydraulic resistance of the channel, ΔP representing the pressure drop and Q the flow rate. Using an energy balance, an expression for the hydraulic resistance in a square channel can be derived[12].

$$R_h = \frac{12\eta L}{1 - 0.63(\frac{H}{W})} \frac{1}{H^3 W} \tag{1.2}$$

With η the viscosity of the fluid and L,H,W the length, height and width of the channel. Figure 1.3 shows some the pressure drop over a bypass channel for some commonly used lengths and flow rates.

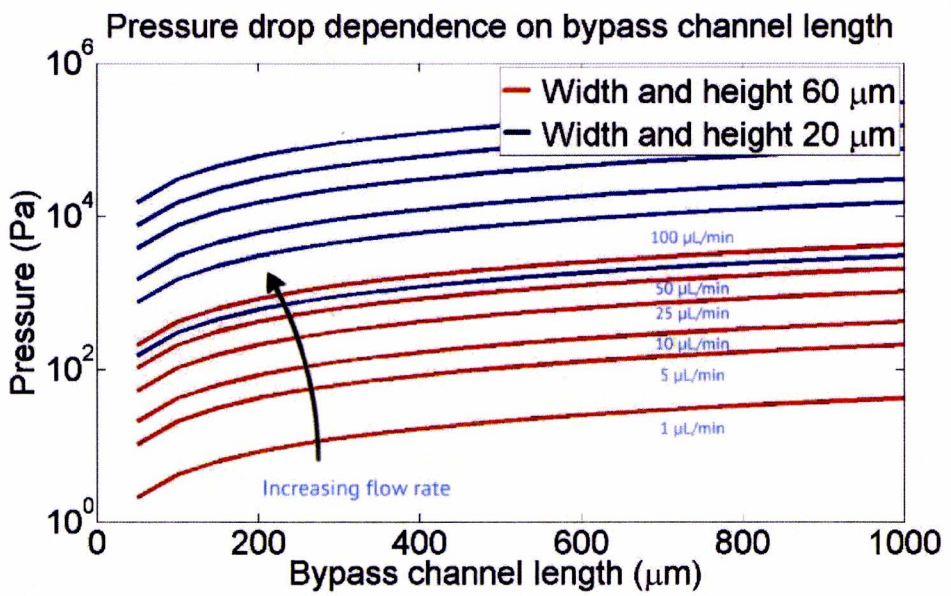

Figure 1.3: Pressure drop dependence on commonly used bypass channel widths, heights and lengths for different flow rates.

Chapter 2

Initial device

2.1 Design

For experiments using the initial design we have performed tests using 50 μm soft beads instead of cells. This was done for several reasons: the beads vary in size between 30-70 μm, representing size differences that may also occur when using cells. A great advantage over cells is that these beads do not require any special protocols regarding medium and treatment, which are necessary for cells. This allows us to use a setup and procedure that are simpler and easier to handle. As the beads are not alive, properties of the beads will not change over time and long experimentation will not influence the outcome, as it would with cells which could for example die during the experiment. Furthermore the chosen beads were readily available. The beads are made of agarose, and some properties of the beads can be found in appendix A .

Now that the bead size is chosen, the trapping area can be designed. A relatively short trapping area was chosen, as this will reduce the hydraulic resistance of the trapping area and, as the hydraulic resistance of the bypass channel is dependent on the resistance of the trapping area, therefore also the length of the bypass channel. The straight part of the trapping area will has a width of 60 μm, while towards the trap the width is reduced to 20 μm over a length of 80 μm. In the entire device a height of 60 μm is used as this should assure all beads to be able to move without being deformed in the wide channels. A segment with these proportions is shown in figure 2.1 .

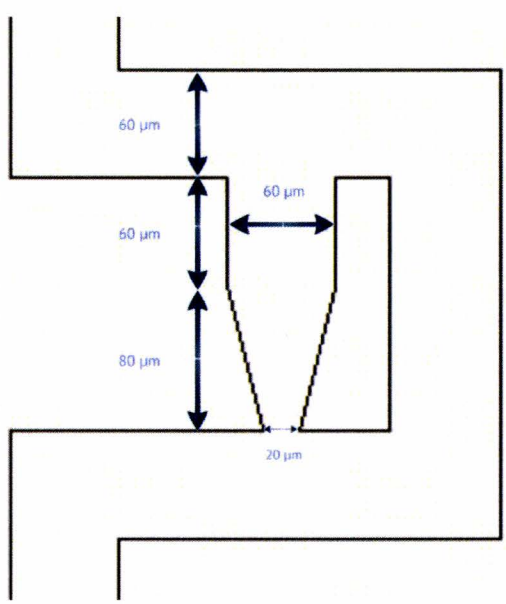

Figure 2.1: A segment with the dimensions of the initial design. General channel width is 60 μm, which decreases to 20 μm in the trapping area. The height of the device is 60 μm.

To determine the sizes of the bypass channel, the hydraulic resistance of the trapping area needs to be known exactly, with and without a bead trapped. In an ideal case, a bead will block the entire trap, causing the hydraulic resistance to go to infinity, ensuring all fluid flow would go to through the bypass channel and making the bypass length irrelevant, as long as its resistance is initially higher than that of an empty trap. However from a practical point of view, this is unlikely to happen for all beads. That is why a rough approximation has been made to ensure a reasonable bypass channel length.

For the approximation, a high leaking area of 25% was chosen. This means that 25% of the cross-sectional area of the trap is not blocked by a bead. Based on that assumption, the new hydraulic resistance was calculated by substituting for the last 50 μm of the trap a height of only 15 μm and doing the hydraulic resistance calculation for an empty trap. This provided us with a range of possible bypass channel lengths between the resistances of an empty trap and a filled trap, which was used to test a number of cells at a range of pressures resulting from this range of resistances. From the calculations it was determined that 40 segments can be placed in series, the first one with a length of 380 μm, stepwise increasing to 1550 μm. In all cases the resistance of the bypass channel is higher than that of the trapping area. For the shortest bypass channel the resistance of the empty trap and the bypass channel are approximately equal, while for the longest bypass channel, the resistance of the bypass channel is close to the resistance of the filled trap approximation.

The range of bypass channel lengths will also help to determine whether the approximation was accurate; if beads are not trapped in certain segments, this would mean that the resistance of the bypass channel was too low and it should be adjusted in a next design. A summary of the lengths and matching resistances can be found in appendix B .

To insert and drain the bead solution two inlets and an exit channel are added to the design, this is shown in figure 2.2a, as well as 3 segments chained together in figure 2.2b .

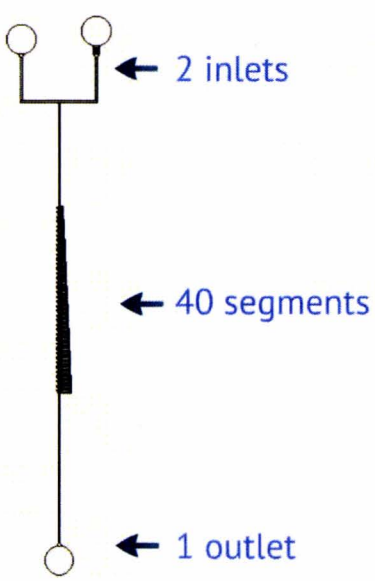

(a) The initial device design with 2 inlets, of which one has a filter, 40 segments and 1 outlet.

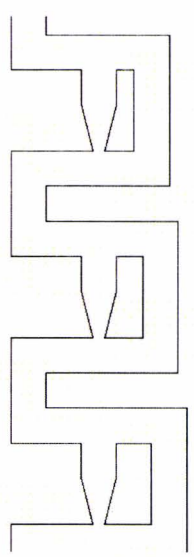

(b) Close-up view of a chain of segments.

Figure 2.2

Having two inlets has several advantages: the bead solution can be entered through one inlet, while the other is used for a medium. This allows regulation of the bead concentration in case the concentration is too high causing clogging to happen. It can also be used to flush debris out of the microfluidic device by blocking the exit manually and having a flow move between the two inlets. A filter is placed in one inlet which may be used to prevent debris or dust from entering the device, in case there is any. The finished design is created using Autocad and sent to a company with a high resolution printer (CAD/Art Services Inc., Bandon, OR (USA)). At this company the design is printed on a transparent polymer sheet with 12000 dpi. This sheet is later used as a mask in the soft lithography process.

2.2 Production

The microfluidic devices, used for the analysis of cells, were made out of polydimethylsiloxane, also known as PDMS. In order to transfer the microstructures of the design into the PDMS, a process known as soft lithography is used. Soft lithography is often used as an inexpensive method to create microstructures. The steps needed are straightforward, but to get an accurate height and width of the structures the process needs to be tuned. The steps taken to create the initial design are can be found in appendices C and D, and are also shown in figure 2.3 .

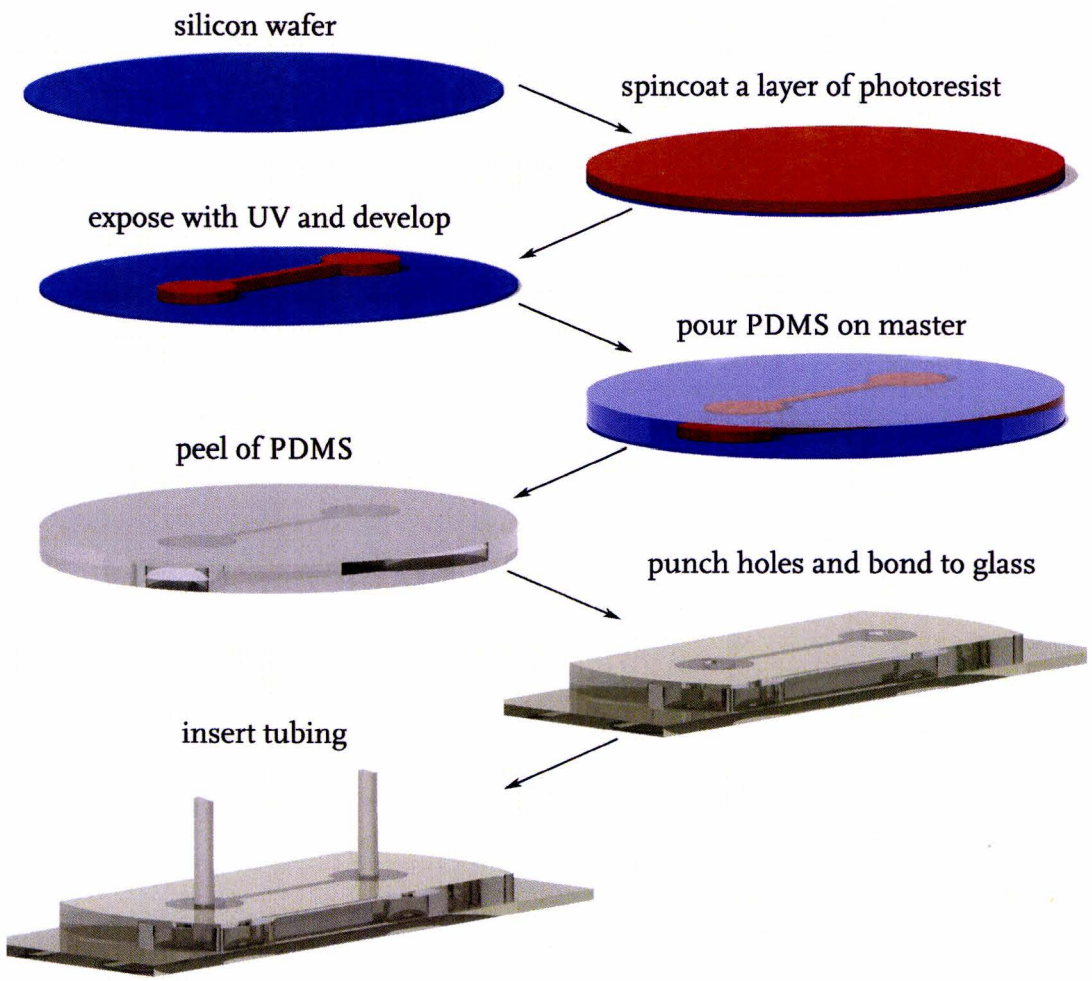

Figure 2.3: The process of creating a microfluidic device using soft lithography. A photoresist layer is added to a silicon wafer, exposed with UV-light and developed to create a microstructures in accordance with the mask design. A PDMS layer is poured on top of this master and cured in order to replicate the features of the master wafer. Holes are punched for the inlets and outlet and the PDMS is attached to a glass microscope slide, finishing the device for usage in experiments [11]

2.3 Setup and protocols

For the experiments with the soft beads, a variety of equipment is used, which can be found in appendix E . The procedure used for the experiment can be found in appendix F . The main goal of this initial experiment is to test if the design, and the trapping mechanism, is functional. A typical result of this experiment is shown in figure 2.4 .

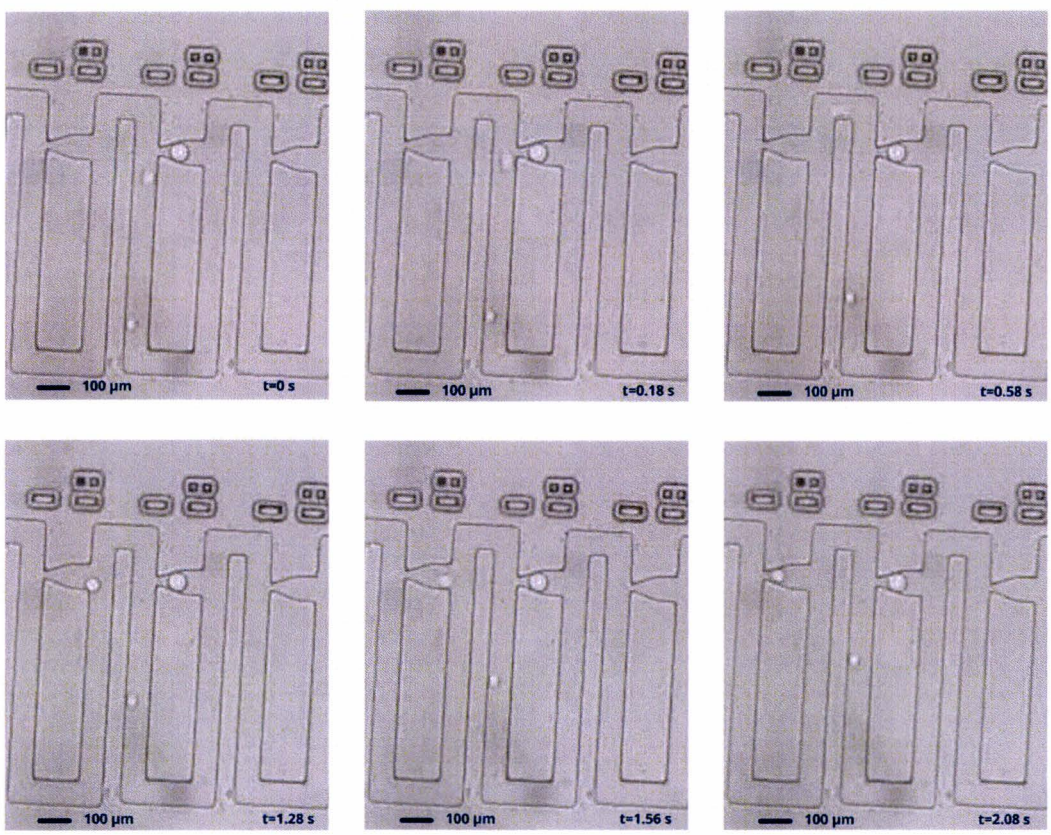

Figure 2.4: An experiment showing the trapping behaviour of the initial design. It shows a bead moving towards a trapping area over the course of 2 seconds, where it gets trapped. The flow in the images is from the right side towards the left side.

2.4 Results

Several observations were made during these experiments: First, it is possible to trap a bead in this device. In most cases, the bead would flow through several bypass channels before it became trapped. The more bypass channels were passed, the closer the bead went towards the trapping area, until it finally moved into the trapping area. The behaviour can therefore be improved by fine-tuning the lengths of the bypass channels towards the observed results and make a new design. In this case, improvements could be made by increasing the general length of the bypass channels.

Second, beads could stick to the surface inside a device and remain there, despite an increase in the flow rate. This occurred with large as well as small beads. This sticking behaviour is most likely due to the adhering properties of the PDMS. It can be prevented by flowing a coating through the device, reducing the adhesion properties of the PDMS.

Third, there were instances that multiple beads got trapped in one trapping area. Up to 3 beads could be seen in a single trapping area. This can be explained by the fact that the used soft beads have a lower deformability that most cells would have. During the experiments the beads deformed little and therefore blocked less of the trap than an easily deformable bead would. The problem could be solved by using more easily deformable beads for the experiment, or by using round channels instead of square ones, but this unfortunately is not possible using the current soft lithography techniques. Another possibility is that the height of the device was as high, especially considering small beads, that the bead was simply not large enough to block the entire floor/ceiling area.

The mentioned observations were taken into account when the final design was made.

Chapter 3

Final device

3.1 Design

For the final design, a choice of cell needs to be made in order to start the design. HL-60 leukaemia cells have been chosen for this purpose. HL-60 cells were originally established from a 36 year old female patient with acute promyelocytic leukaemia [13].

HL-60 cells have been used extensively as a model of how certain types of blood cells are formed [14]. This means there is an abundance of literature about these cells from a biological aspect, as well as experiments on mechanical properties. This data can be used to compare the results of the experiments with the known data and determine device accuracy.

The doubling time of HL-60 cells is approximately 48 hours, making it simple to maintain a sufficient supply of these cells for the experiments. The size of the HL-60 cells is around 11-13 μm [14], which means that the dimensions of the initial design needed to be adjusted.

This adjustment has been made by reducing the width and height to 20 μm. This is slightly larger than the cells size, a choice that has been made to reduce the pressure drop over the entire device. Trap width has been chosen to be 6 μm, with the same lengths for the straight and sloped areas of the trap. This small size will cause a cell to block a larger area of the trap, preventing multiple cells from entering the trap.

A new feature of this design is the addition of extra trapping areas. In the initial design, a segment consisted of an inlet, the trapping area and bypass channel, and an outlet. The space between this segment outlet and inlet is now used to create another bypass channel, increasing the amount of cells that can be tested to 79 while not creating an additional pressure drop. A few segments are shown in figure 3.1.

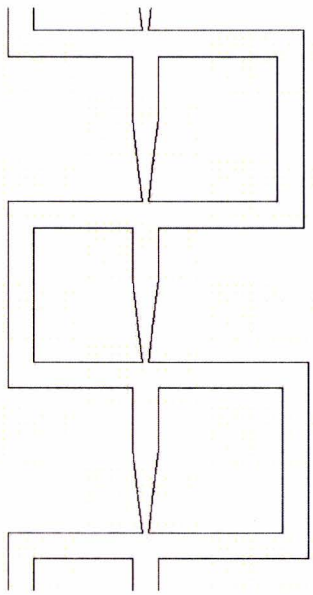

Figure 3.1: A few segments of the final design. The main difference with the initial design is that an extra trapping area has been added between the outlet and inlet of two segments, allowing a single device to have 79 trapping areas.

The hydraulic resistance of the bypass channels for the 39 added trapping areas has been chosen constant, while the bypass channels for the 40 initial trapping areas are steadily increasing in resistance. The constant length of the new bypass channels allows us to study cells under identical conditions, while the variation in length of the initial bypass channels allows measurement of different pressures at a constant flow rate. A constant flow rate is important as variations in flow rate take a while to stabilize and hence increase experimentation time. Lengths and matching resistances can be found in appendix B.

3.2 Setup and protocols

For the experiments with the cells, the setup is mostly identical to the initial design setup, with some additions which can be found in appendix E. The experimental procedure consists of applying a coating to reduce the adhesion properties of the PDMS, followed by several other preparation steps which can be found in appendix G. The goal of this experiment is to observe the trapped cells and determine the mechanical properties based on this observation. Cells are trapped in the device at a low flow rate, then subjected to a stepwise increase in flow rate until all cells have squeezed through their traps and left the device. This process is recorded with a camera to create movies of the cells at each flow rate.

3.3 Results

After completing a full experiment with identical cells at different flow rates, which takes around 45-90 minutes, the movies are split into frames using Windows movie maker. These frames are browsed to find a clear frame of each trap. For each trapped cell there is a critical pressure, above which the cell will squeeze through the constriction and get released from the trap. This critical pressure depends on the mechanical properties of the cell as well as on the ratio between the size of the cells and the width of the constriction. The presence of cells within the traps as a function of the pressure difference across each trap can thus be used as a measure of the mechanical properties of the cells. Additionally, at each pressure, the shape of cells in the traps can also be analysed to acquire info about the cell such as the cortical tension, using the liquid drop model, as well as the original size of the cell.

3.3.1 Critical pressure

To determine the critical pressure of a cell it is sufficient to know at which flow rate the cell squeezed through the trap and at which segment this occurred. Since the critical pressure is defined as the pressure at which a cell is just able to squeeze through a trap, the critical flow rate is the flow rate at the time this happened. To acquire information about the critical pressure and flow rate it is not necessary to track changes in shape and volume, only the presence of a cell, and hence it is not very time consuming to determine the critical pressure for many cells. Figure 3.2 shows an example of a cell that squeezes through at a critical flow rate.

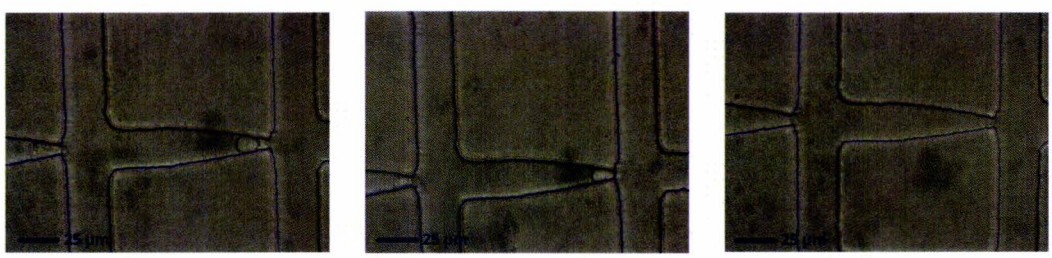

Figure 3.2: A cell is squeezed through a trap at a critical flow rate. The flow is from the left side to the right side. From left to right, the flow rates are 0.5, 1 and 1.5 μL/min.

Acquiring this data from three separate experiments, we are able to create figure 3.3 .

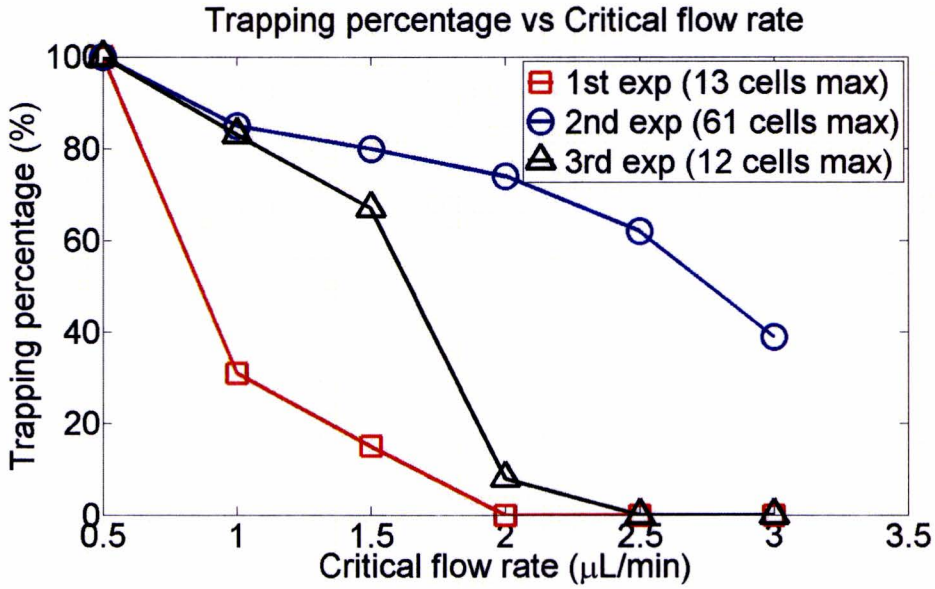

Figure 3.3: The percentage of trapped cells plotted versus the critical flow rate at which they squeezed through the traps. The first experiment started with 13 cells in the trapping areas, the second with 61 cells and the third with 12 cells. Experiments one and three show a clear steep descend in trapping percentage while the second experiment shows a gentler and constant descent.

Three experiments were done with the same protocol as described in the experimental steps section. The figure shows what percentage of the total number of initially trapped cells was still in a trap at the time the flow rate was increased. In the first experiments, 13 cells were trapped, in the second 61 cells and in the third 12 cells. The first experiment initially shows a steep decline from 100% to 30% over the course of a single flow rate increment step. At higher flow rates cells continue to squeeze through the traps but the reduction in the number of trapped cells is much less pronounced, decreasing in an approximately linear fashion as function of the applied flow rate. The second experiment does not show a steep decline at all, as here cells squeeze through the traps a couple at a time with each flow rate increment step. The third experiment shows a linear squeezing through of the cells at the start, but then a steep decline from 70% to 10%. If we look at the shape of the graphs, the first and the third experiment look very alike. Both show the steep decline, only at different flow rates. The second experiment does not have this decline, but in that experiment there were overall much more cells in the traps, more than the other two experiments combined, resulting in a more equal spread of the different types and sizes of HL-60 cells.

Although it is useful to consider the critical flow rate, the critical pressure supplies more accurate information, as the segments have different pressure drops with the same flow rate because of the different hydraulic resistances. These pressure drops are shown in figure 3.4 .

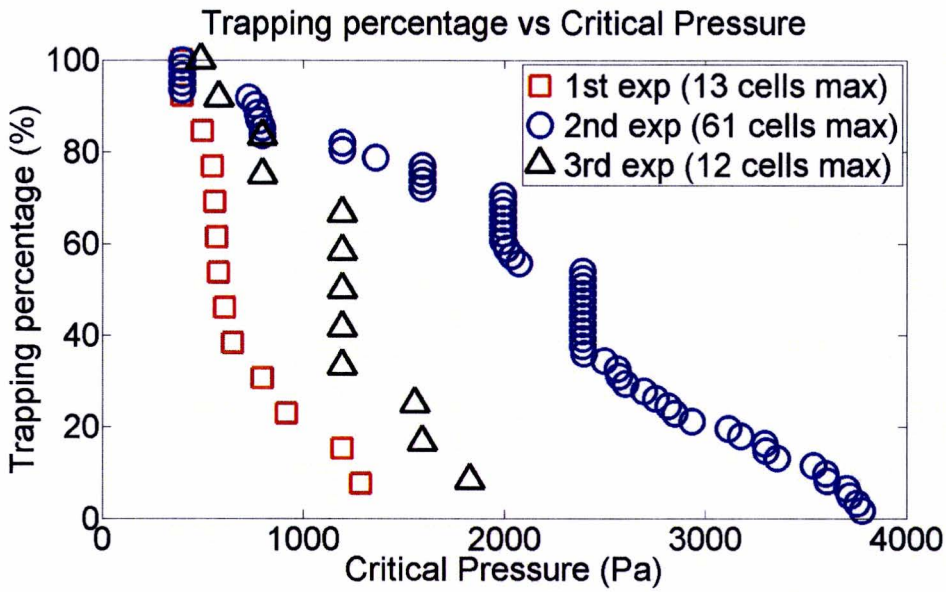

Figure 3.4: The percentage of trapped cells plotted versus the critical pressure at which they squeezed through the traps. The first experiment started with 13 cells in the trapping areas, the second with 61 cells and the third with 12 cells. All experiments have a common shape; a steady decline followed by a rapid drop followed by a steady decline.

Each symbol in the graph represents a cell squeezing through its trap. When we look at the curves of the experiments, we see that all have a common shape. At low pressures there is a steady but slow decline, followed by a rapid drop of the amount of cells in the trap. After this drop the cells start going through the traps at a steady rate again. This is shown in figure 3.5 .

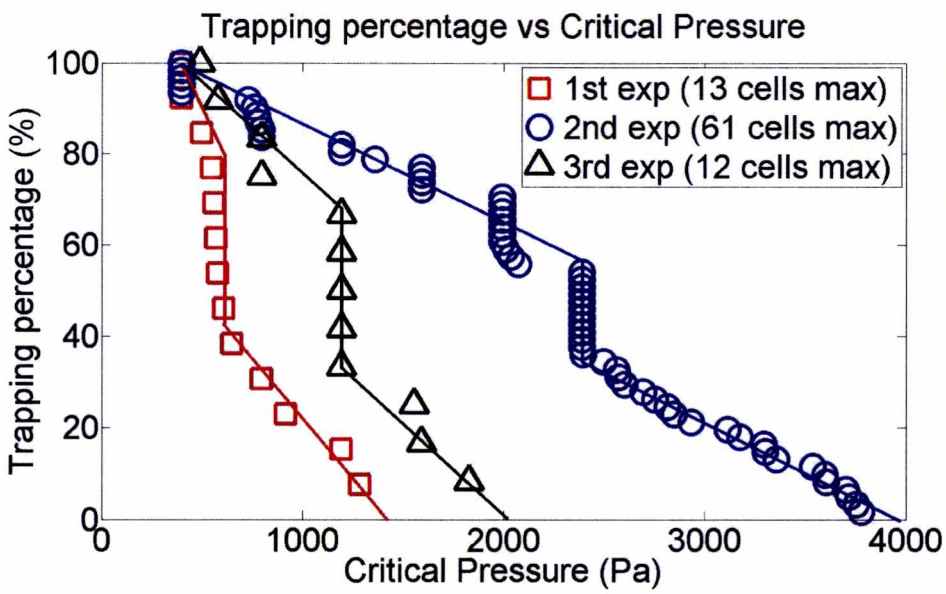

Figure 3.5: The percentage of trapped cells plotted versus the critical pressure at which they squeezed through the traps. The first experiment started with 13 cells in the trapping areas, the second with 61 cells and the third with 12 cells. All experiments have a common shape; a steady decline followed by a rapid drop followed by a steady decline. This common shape is shown by the hand-drawn lines through the data points.

Although the pressures at which the rapid drop happens are different, it happens around the same percentage of trapped cells: 40-70%. The critical pressure regime where this happens could therefore be a good indicator for the properties of a cell. The critical pressure itself however varies a lot between these experiments. Several reasons for this observed lack of reproducibility were observed in the experiments, as well as other observations.

First, the pressures calculated assumed perfect conditions. However, during all three experiments a part of the flow went from the first inlet to the second inlet, despite the fact it was sealed by the sealing clip. This was visible by looking at the intersection between the inlets. Also, during the experiments liquid appeared around the PBS inlet connector, thus indicating that the device was not perfectly sealed and the flows in the device were lower than those applied with the syringe pump. It was unclear how much flow was exactly lost this way, resulting in an unknown flow rate correction that we estimate to be on the order of 10-50%, based on observations in the movies. For different devices and different experiments, the thereby induced error in the flow rates could have varied significantly, thus possibly accounting for the observed lack of reproducibility observed for our experiments.

Second, cell conditions may not have been fully identical. Experiments were done with a week in between, in which the cells may have changed mechanical properties during proliferation. The preparation time for the experiments also varied and a full experiment took between 45 and 90 minutes. In this time the cells were out of the incubator so the temperature, humidity, CO_2 and O_2 were not regulated during this time. This causes the cell to die over the course of experimentation time and can affect the mechanical strength of the cells resulting in a lack of reproducibility observed in the experiments.

Third, the channel and trap sizes of the silicon master were not exactly identical to the design. Using a profilometer, the height was determined to be 22 μm instead of 20, while the channel width was around 30 μm instead of 25. The width of the trap tip was around 8 μm instead of 6 μm. These different sizes result in a lower hydraulic resistance, which causes a lower pressure. However, since all devices were made with the same wafer, this applies to all the experiments equally and should therefore not have been the reason for the difference between the different experiments.

Fourth, when using the hydraulic resistance to calculate the pressure drop over a cell, we assumed the cell would block the entire trapping area. However, because the height and width of the trapping area compared to the cell diameter are too large, a cell will in most cases not be able to block the entire trapping area. This means not all flow will go through the bypass channel but instead some will go through the trapping area, resulting in a lower pressure drop over the bypass channel and hence the cell will be subjected to a pressure that is actually lower than calculated. Whether or not this effect occurs is dependent on the exact geometry of a trapping area (as none are identical due to the production process) and the size of the cell (as larger cells will block more of the trap). This does not explain the lack of reproducibility of the experiments, but, as with the third observation, shows that the pressures shown in the figure are higher than the actual pressures as experienced by the cells.

3.3.2 Shape analysis

In order to use the shape to measure an intrinsic property such as deformability, information about that shape in combination with a model of the deformation process is needed[3]. There are several mechanical models to describe the mechanical behaviour of cells, with varying degrees of complexity, such as cortical shell-liquid core (or liquid drop), which is widely applied to suspended cells, or the solid model, which is generally used for adherent cells. The power-law structural damping model is more suited for studying the dynamic behavior of adherent cells, while the biphasic model has been widely used to study musculoskeletal cell mechanics[16]. The mechanical properties of the cells can also be described using a homogeneous linear viscoelastic solid model (LVS). Since there is such a wide variety of model, the liquid drop model has been chosen as this applies to most circulating cells, while also being not overly complex. However, this lack of complexity also means this model may not describe the cell behavior as accurate as other, more advances models.

Liquid drop model

Cells which can be characterized by the liquid drop model remain spherical in shape when suspended due to a constant surface tension, also called cortical tension[14]. The model has often been used for micropipette aspiration where it describes how cells can deform continuously into a micropipette with much smaller diameters when the suction pressure exceeds a certain threshold pressure. This threshold pressure is also referred to as critical pressure, which is defined as the moment when a projection of the cell is formed inside the pipette with a radius equal to the radius of the pipette tip. An excess pressure beyond this point will cause the cell to flow completely and continuously into the pipette. The critical pressure can be determined using the Young-Laplace equation, which relates the surface tension of the cell membrane to the pressure difference between inside and outside of the cell by the radius of curvature. Important to notice is that our liquid drop model assumes that the volume of the cell does not change during the experiment. In our device, we do not suck in the cell through the trap as with micropipette aspiration, but reverse the process and attempt to push the cell out of the trap. However, the liquid drop model is still valid. The critical pressure now relates to the moment where a projection of the cell is formed out of the trap with the diameter of the trap width. A top view of this is shown in figure 3.6 .

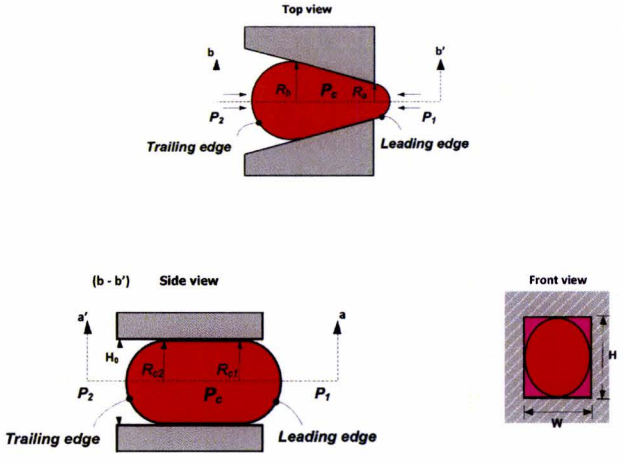

Figure 3.6: Top view, side view and front view of the maximum-volume model of a cell in a trap. The volumes consist of a half-spheroid for the trailing edge and leading edge and an extended trapezoid for the middle section, shown in magenta in the front view.

Cell shape model

In order to make a good approximation for the cortical tension, we need to have a realistic cell shape model. Figure 3.6 shows a possible model. This model assumes the cell is touching the sides of the trap as well as the floor and ceiling. The trailing and leading edges can be described as half-spheroids, with radii Ra and $Rc1$ for the leading edge, and Rb and $Tc2$ for the trailing edge, while the middle section is assumed to be an extended trapezoid with lower length $2Rb$ and upper length $2Ra$. However, as the height of our device is 22 μm while cell diameter is around 12-13 μm, this model would not be an accurate representation of what occurs during experiments, as the cell cannot be stretched enough in the vertical direction to reach both floor and ceiling. This model overestimates the total volume of the cell and will therefore be called the maximum-volume model.

Figure 3.7 shows a different model, this one describing the trailing and leading edges as half-spheres with radii R_a and R_b respectively (thus R_c1 equals R_a and R_c2 equals R_b in comparison with the previous model). The middle section is modelled as a frustum of a cone (a flat top) with lower radius R_b and upper radius R_a. This model calculates the minimum of the volume the cell while in the trap, underestimating the volume as in reality the middle section is more of a spherical shape then cone-like due to the surface tension. This model will be called the minimum-volume model.

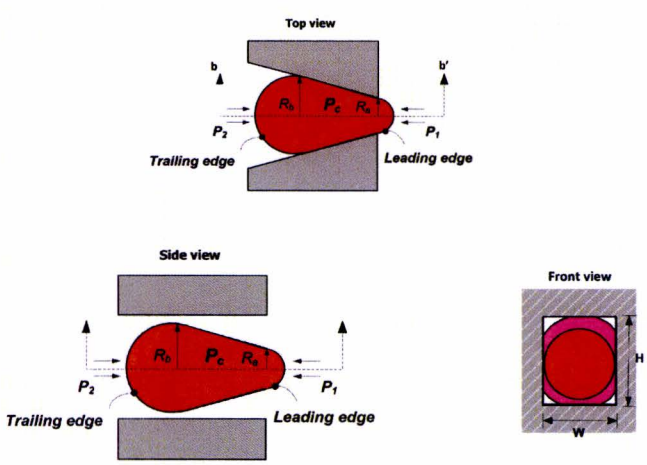

Figure 3.7: Top view, side view and front view of the minimum-volume model of a cell in a trap. The volumes consist of a half-spheres for the trailing edge and leading edge and a frustum of a cone for the middle section, shown in magenta in the front view.

As it is not possible with a normal microscope to observe the side view of a cell in a trap, an assumption must be made about its shape. The total volume of the cell will be between the minimum-volume and maximum-volume model. Both will be used in the calculations for the cortical tension and the original cell size.

Cortical tension

Maximum-volume model

We start the calculation of the cortical tension by assuming the half-spheroids of the maximum-volume model for the trailing and leading edge, shown in figure 3.6. P_c represents the internal pressure of a cell, while P_1 and P_2 are the pressures at the trailing edge and the leading edge of the cell. Radii of interest are the trailing edge and leading edge radii of the cell as can be seen from a top view and that are limited by the geometry of the walls, R_a and R_b, as well as the trailing edge and leading edge radii as can be seen from a side view and that are limited by the floor and ceiling of the channel, R_{c1} and R_{c2}. The internal pressure of a cell, with respect to the leading edge and using the Young-Laplace formula, can be described as

$$P_c = P_1 - T_c(\frac{1}{R_{c1}} + \frac{1}{R_a}) \tag{3.1}$$

With T_c the cortical tension of the cell. Likewise, the internal pressure can be described with respect to the trailing edge of the cell, which is

$$P_c = P_2 - T_c(\frac{1}{R_{c2}} + \frac{1}{R_b}) \tag{3.2}$$

Combining these two formulas, the applied pressure on both sections of the cell can now be described as

$$P_2 - P_1 = T_c(\frac{1}{R_{c1}} + \frac{1}{R_a} - \frac{1}{R_{c2}} - \frac{1}{R_b}) \tag{3.3}$$

For the maximum-volume model, the height of the channel is identical for the leading and trailing edge of the cell, which causes R_{c1} and R_{c2} to be identical, as both are equal to half the channel height H. This simplifies the applied pressure to

$$P_2 - P_1 = T_c(\frac{1}{R_a} - \frac{1}{R_b}) \tag{3.4}$$

Minimum-volume model

For the minimum-volume model, we start the calculation of the cortical tension by assuming the half-spheres of the minimum-volume model as shown in figure 3.7 . The applied pressure on the trailing and leading edge of the cell can still be described with formula 3.3 .

For the minimum-volume model however, R_{c1} equals R_a and R_{c2} equals R_b, therefore the formula becomes

$$P_2 - P_1 = T_c(\frac{1}{R_{c1}} + \frac{1}{R_a} - \frac{1}{R_{c2}} - \frac{1}{R_b}) = T_c(\frac{2}{R_a} - \frac{2}{R_b}) = 2T_c(\frac{1}{R_a} - \frac{1}{R_b}) \tag{3.5}$$

Calculation and comparison

In order to determine R_a and R_b, six points are chosen in an image of a cell, three for each edge. Two points are taken at the location at which the edge of the cell connects with the trap wall, and the last point is taken on the curve of the cell edge, as far away from the centre of the cell as possible. This is shown in figure 3.8 . R_a is determined as the average of the half the distance between point 1 and 2, and the horizontal distance between point 2 and 3. R_b is likewise determined as the average of the half the distance between point 4 and 5, and the horizontal distance between point 5 and 6. Together with the pressure drop, which can be derived from knowing the trap number (and hence the hydraulic resistance) and the flow rate, the cortical tension can now be calculated, and this is done for 10 cells at different flow rates of which the averages are shown in table 1.

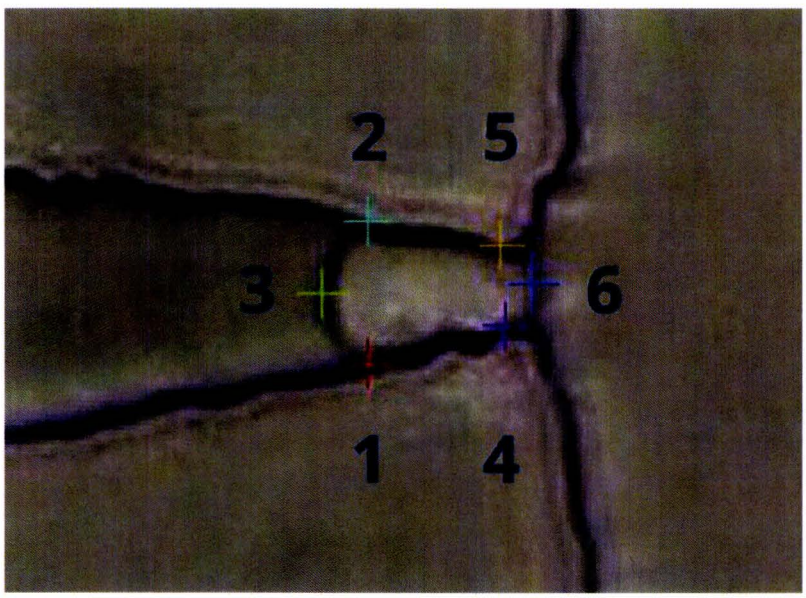

Figure 3.8: The six point method, which is used to gain information about the geometry of the cell. With these points the cortical tension and original volume can be calculated.

Table 1: Cortical tension calculations at various flow rates		
Maximum-volume model		
Flow rate (µL/min)	Average cortical tension (pN/µm)	Standard deviation (pN/µm)
0.5	$1.3 \cdot 10^3$	$7.5 \cdot 10^2$
1	$2.4 \cdot 10^3$	$1.5 \cdot 10^3$
1.5	$4.0 \cdot 10^3$	$2.5 \cdot 10^3$
2	$5.7 \cdot 10^3$	$5.4 \cdot 10^3$
2.5	$12.2 \cdot 10^3$	$13.5 \cdot 10^3$
3	$10.2 \cdot 10^3$	$10.3 \cdot 10^3$
Minimum-volume model		
Flow rate (µL/min)	Average cortical tension (pN/µm)	Standard deviation (pN/µm)
0.5	$6.4 \cdot 10^2$	$3.7 \cdot 10^2$
1	$1.2 \cdot 10^3$	$7.4 \cdot 10^2$
1.5	$2.0 \cdot 10^3$	$1.2 \cdot 10^3$
2	$2.9 \cdot 10^3$	$2.7 \cdot 10^3$
2.5	$6.0 \cdot 10^3$	$6.8 \cdot 10^3$
3	$4.1 \cdot 10^3$	$2.2 \cdot 10^3$

According to literature[14] the cortical tension of HL-60 cells is around 155 $\pm$ 81 pN/μm. This means the calculated cortical tension of the maximum-volume model is approximately 10 times larger, while the minimum-volume model is approximately 5 times larger. A possible explanation is the deviation of the actual pressure from the calculated one due to leaking as explained in the previous section, which would lower the cortical tension. Another explanation is the deviation of the geometry of the cell from both models , which is possible since the models assume a spheroid and a spherical shape, while the trap outlet is shaped as a rectangle.

Original size calculation

To determine the original size of a cell, we estimate its volume in its deformed state and use this information to determine the original volume. As with the cortical tension, we will do this for the maximum-volume model as well as the minimum-volume model.

Maximum-volume model

For the maximum-volume model, the volume of the cell can be determined by calculating and summing up the volumes of three separate areas: a half-ellipsoid for the trailing edge of the cell, an extended trapezoid for the middle section and another half-ellipsoid for the leading edge of the cell. These three areas are visible in figure 3.6 . The total volume is equal to the cell in its original state, as no volume is lost or gained during deformation in accordance with the liquid drop model we have chosen. We assume that, in its original state, the cell assumes a spherical shape.

Volumes for these geometries are derived from basic mathematics, and are shown below[15] .

$$V_{ellipsoid} = \frac{4}{3}\pi r_1^2 r_2 \tag{3.6}$$

$$V_{extendedtrapezoid} = \frac{HL_{mid}}{2}(b_{lower} + b_{upper}) \tag{3.7}$$

$$V_{sphere} = \frac{4}{3}\pi r^3 \tag{3.8}$$

With these formulas, the total volume of the cell can be described as

$$V_{tot} = V_1 + V_2 + V_3 \tag{3.9}$$

$$V_{tot} = \frac{1}{2}\frac{4}{3}\pi R_a^2 \frac{1}{2}H + \frac{HL_{mid}}{2}(2R_a + 2R_b) + \frac{1}{2}\frac{4}{3}\pi R_b^2 \frac{1}{2}H \tag{3.10}$$

$$V_{tot} = \frac{H}{3}\pi R_a^2 + HL_{mid}(R_a + R_b) + \frac{H}{3}\pi R_b^2 \tag{3.11}$$

With H the height of the device and L_mid the length between the two outer volume sections. By taking the volume of a sphere for the original volume, the original diameter of the cell can be derived:

$$\frac{4}{3}\pi R_0^3 = \frac{H}{3}\pi R_a^2 + HL_{mid}(R_a + R_b) + \frac{H}{3}\pi R_b^2 \tag{3.12}$$

$$D_cell = 2R_0 = 2[\frac{1}{4}H(R_a^2 + R_b^2 + \frac{3HL_{mid}(R_a + R_b)}{\pi})]^{\frac{1}{3}} \tag{3.13}$$

Minimum-volume model

The minimum-volume model also sums up the volumes of the trailing edge, leading edge and middle area. In this case we have a half-sphere for the trailing edge of the cell, a frustum of a cone for the middle section and another half-sphere for the leading edge of the cell. The volume of the middle section can be described as

$$V_{frustumcone}) = \frac{\pi L_{mid}}{3}(R_a^2 + R_b^2 + R_a R_b) \tag{3.14}$$

Deriving the original volume, this becomes

$$\frac{4}{3}\pi R_0^3 = \frac{2}{3}\pi R_a^3 + \frac{\pi L_{mid}}{3}(R_a^2 + R_b^2 + R_a R_b) + \frac{2}{3}\pi R_b^3 \tag{3.15}$$

This means the original cell diameter can be calculated using

$$D_{cell} = 2R_0 = 2[\frac{1}{2}(R_a^3 + R_b^3) + \frac{1}{4}L_{mid}(R_a^2 + R_b^2 + R_a R_b)]^{\frac{1}{3}} \tag{3.16}$$

Calculation and comparison

Using the six point method described in the cortical tension section, we know R_a and R_b for all cells. The length L_{mid} is determined by taking the distance between point 1 and 4. We can plot this cell diameter for both volume models against the critical pressure at which a cell is flown through a trap, these are shown in figure 3.9.

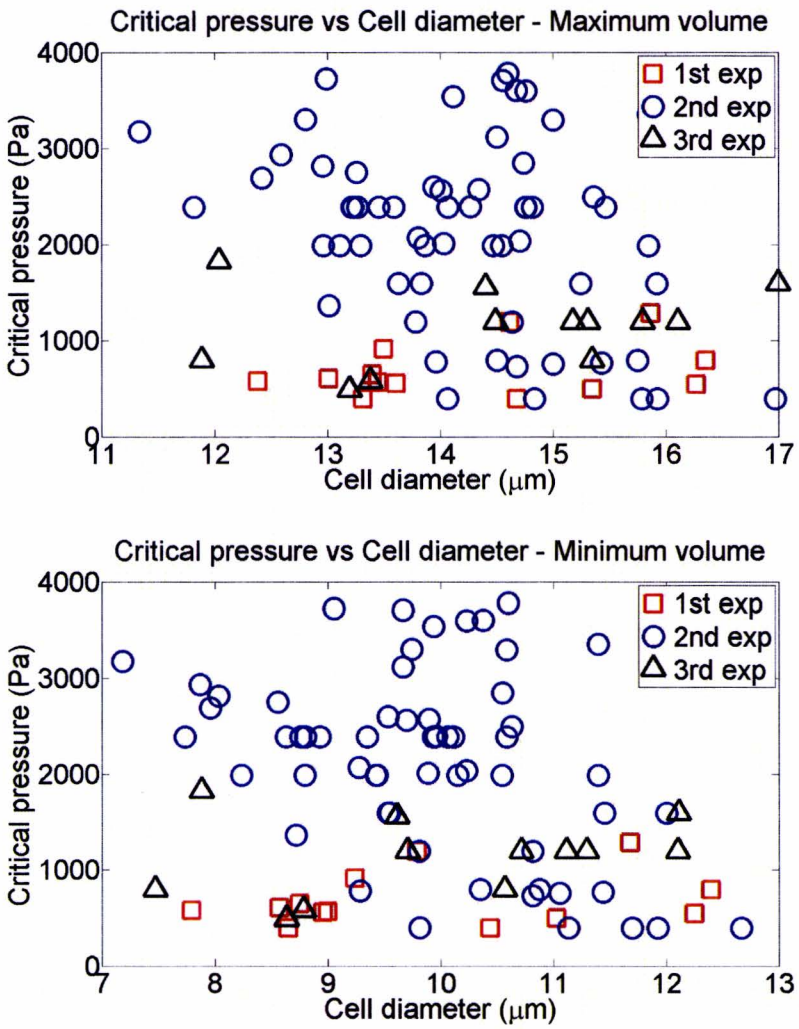

Figure 3.9: These figures shows the cell diameters of the cells that squeeze through a trap at their critical pressure. The diameters are determined using the six point method and the top image show the diameters calculated using the maximum-volume model,while the lower image shows the diameter calculated using the minimum-volume method.

For the maximum volume, there is a clear spread of cell diameters with most between 12-16 μm. For the minimum volume these cell diameter are between 8-12 μm. Taking the average, we can assume the original cell diameter is around 12 ± 2 μm. This is in agreement with the size range described in literature, which is 12.4 ± 1.2 μm[14]. The graphs show that there is no clear connection between cell size and the critical pressure. This is unexpected, as larger cells need to be deformed more in order to squeeze through a trap, and therefore can be expected to have a higher critical pressure.

Chapter 4

Conclusion and suggestions

In this project we propose a new device and approach to determine the mechanical properties of cells in larger quantities. The device contains multiple cell traps, in which cells can be trapped and deformed simultaneously. The cells deform when the pressure is increased until he cells squeeze through their traps when a critical pressure is applied. To test its effectiveness, HL-60 cells were analysed using the device. The critical pressure, the cortical tension and the cell diameter dependence were determined. The critical pressure curves, obtained from different repeats of the same experiment, were identical in shape, but the exact values of the critical pressure regime, at which the curves steeply drop and many cells squeeze through their traps at once, varied substantially. This lack of reproducibility might be attributed to leakage from one inlet to the other and/or by changes in cell properties in the time frame between the experiments. The results however also indicate that the critical pressure regime might be used as a mechanical property indicator in future experiments. The cortical tension that was calculated using the liquid drop model was approximately five to ten times larger than typical values reported in literature. Also no systematic dependence of the critical pressure on the cell diameter was observed. Both these observations might be explained by the leakage and time-dependent property changes mentioned above. The problems that may have caused these outcomes can however be addressed in future device design. Several improvements to the design can be made:

To increase the accuracy of the geometry of the new design, the lithography process need to be improved. Despite efforts to reduce the distance between mask and wafer, dimensions of the channels on the wafer were not identical to the dimensions of the design. A pre-adjusted mask (with smaller channels then intended), a different photoresist and different exposure times are all possibilities that might improve the step from design dimensions to wafer dimension, which is especially important for the trap tip diameter.

During the experiments, there were some problems regarding the setup of the experiment. These problems include cells not being able to reach the trapping areas and debris clogging the device though the inlet. The latter is mainly a problem of dimensions. The channel from an inlet of the device to the first trap has a width of 100 μm and a length of 12.5 mm. The tubing has a relatively large diameter of 0.86 mm. While filling these with cell solution, using the syringe pump and a low flow rate, the speed of the fluid is low as well because of the large dimension of the tubing and inlet area. It is low enough that either cells sediment to the bottom and do not reach the trapping areas, or that the experimentation time would take too long. When the flow rate is increased to have the cells move at a rate at which they do not sediment in the wide areas, the cells pressure drop over the bypass channels is too large for the cells to remain in the traps and they will squeeze through. The solution to this problem is to redesign the device to have smaller inlet channels. Although this increases the pressure drop over the entire device it will increase the flow velocity at identical flow rate and therefore sedimentation should no long play an important role.

The debris clogging the inlet can be prevented by using a better (sharper) puncher to create the inlets which does not cause microscopic debris. After the punching is done, the inlets of the PDMS device can be cleaned using PBS before it is attached to the glass slide.

While doing the experiments, many trapping areas did not contain cells. This is probably because the dimensions of the actual devices differ from the design, resulting in a different hydraulic resistance for the trapping areas and the bypass channels. To correct for this, a new design could

be made in which the hydraulic resistance of the bypass is decreased even more in relation to the resistance of the trapping area.

The calculation of the critical pressure showed much variation between experiments that should have been reproducible. To improve on the conditions of the experiments, several options are available:

- The entire setup can be placed in an incubator. This will make sure the cells stay alive and the properties of the cells do not change over the course of the experiment.
- Instead of using a plastic syringe as used in these experiments, a glass syringe could be used to improve the steadiness of the flow.
- To correct for the fact that cells do not completely close off a trapping area when trapped, the device design can be adjusted to have a lower height, but keeping in mind that the height must be at least the height of a cell so it can move through the device without deforming.

The liquid drop model used for the shape analysis may be changed to a more complex model to get more accurate values for the changes is geometry.

The leaking through the second inlet was most apparent at higher pressures. In case it can not be prevented entirely, using larger cells for analysation will cause the overall hydraulic resistance to decrease (as channels are wider) and reduce the influence of this leakage.

When all the improvements are implemented some of the first future experiments can be done with Hl-60 cells treated with cyto-D. In that way the device can be used to a test its ability to measure the difference in mechanical properties while also maintaining the device dimensions. Once optimized the resulting device can be used for not only the Hl-60 cells but also for other types of cells such as cancer cells, and may one day be used as a reliable method to screen for diseases.

Bibliography

[1] ElizabethArias Ph.D. KennethD.Kochanek M.A. Sherry L.Murphy B.S. BettyL.Smith B.S.Ed. DivisionofVitalStatistics Arialdi M.Minino, M.P.H. Deaths: Final data for 2000. *NationalVital Statistics Report*, 50(15), September 16, 2002. 1

[2] http://www.cancer.gov/cancertopics/pdq/screening/overview/Patient National Cancer institute. 1

[3] Quan Guo. Microfluidic device for measuring the deformability of single cells. B.Sc., Zhejiang University, Hangzhou, China, 2012. 2, 3, 5, 22

[4] Patrick Anderson Carlijn Bouten Agnese Ravetto, Jaap den Toonder. Mechanical screening and selection of circulating cells. 2009. Poster. 1

[5] http://www.stanford.edu/group/blocklab/OpticalStanford university. 2

[6] Robert M. Hochmuth. Micropipette aspiration of living cells. *Journal of Biomechanics*, 33(15-22), 2000. 3

[7] http://www3.imperial.ac.uk/singlecellanalysis/technologies/cellmanipulation/micropipette. 3

[8] Elisa Melead Hans M. Wyss, Thomas Franke and David A. Weitz. Capillary micromechanics: Measuring the elasticity of microscopic soft objects. *The Royal Society of Chemistry, soft matter*, 6:4550?4555, June 2010. 3

[9] Igor Sokolov. Atomic force microscopy in cancer cell research. *Cancer Nanotechnology*, pages 11–17, 2007. 4

[10] http://www3.physik.uni greifswald.de/method/afm/eafm.htm. 4, 5

[11] Jelle J.F. Sleeboom. Trapping and squeezing in a microfluidic device: Viscoelastic behavior of microgels via osmotic shock measurements. July 19 2012. 7, 8, 13

[12] Henrik Bruus. Theoretical microfluidics. *MIC - Department of Micro and Nanotechnology, Technical University of Denmark*, 2005. Lecture notes. 9

[13] J Trujillo K McCredie M Ahearn S Tsai R Metzgar G Aulakh R Ting F Ruscetti R Gallagher, S Collins and R Gallo. Characterization of the continuous, differentiating myeloid cell line (hl-60)from a patient with acute promyelocytic leukemia. *Blood (print ISSN 0006-4971, online ISSN 1528-0020)*, 2011. 16

[14] Wilbur A. Lam Michael J. Rosenbluth and Daniel A. Fletcher. Force microscopy of nonadherent cells: A comparison of leukemia cell deformability. *Biophysical Journal*, 90(8):2994?3003, January 2006. 16, 22, 26, 29

[15] http://mathworld.wolfram.com. 27

[16] Quek ST. Lim CT, Zhou EH. Mechanical models for living cells–a review. *J Biomech*, 39(2):195–216, 2006. 22

Appendix A

Information about the agarose beads

Product name and company	Workbead 40/10000, Bio-Works, Sweden
Diameter	30-70 μm with an average of 50 μm
Density	1200 g/m^3

Additional information can be found on the company's website, http://www.bio-works.net/workbeads4010000se

Appendix B

Design dimensions and resistances

Table 2: Initial design sizes and resistances	
General (µm)	
Height	60
Width	60
Trap (µm)	
Trap tip width	20
Trap length	80
Straight area	60
Bypass channel length (µm)	
Lowest	380
Highest	1550
Hydraulic Resistance $(\frac{Pa \cdot s}{m^3})$	
Empty trap	$8.16 \cdot 10^{11}$
Filled trap	$9.77 \cdot 10^{12}$
Shortest bypass	$9.50 \cdot 10^{11}$
Longest bypass	$3.88 \cdot 10^{12}$

Table 3: Final design sizes and resistances	
General (µm)	
Height	20
Width	20
Trap (µm)	
Trap tip width	6
Trap length	80
Straight area	60
Bypass channel length (µm)	
Lowest	425
Highest	825
Hydraulic Resistance $(\frac{Pa \cdot s}{m^3})$	
Empty trap	$4.49 \cdot 10^{13}$
Filled trap	$1.03 \cdot 10^{15}$
Equal length bypass	$7.13 \cdot 10^{13}$
Shortest bypass	$7.68 \cdot 10^{13}$
Longest bypass	$1.49 \cdot 10^{14}$

Appendix C

Creating a master wafer using soft lithography

1. A 5 inch silicon wafer is taken from its storage container and its surface is cleaned using compressed nitrogen air. The wafer is placed on the spincoater, a device capable of rotating the wafer at high speeds.

2. A small amount of photoresist (microchem su-8 2050) is poured on top of the wafer and the spincoater is set to a specific time and speed, which will influence the thickness of the SU-8 layer. For the initial design, these values were 500 RPM for 10 seconds followed by 1500 RPM for 30 seconds. After spinning the wafer is transferred to a hotplate for 3 minutes, which is set to 65 °C. Afterwards the temperature is raised to 95 °C for 6 minutes, followed by a cooling down to room temperature. This step is called the soft bake and is used to evaporate residual solvent.

3. The mask with the device design is placed on top of the wafer. A glass plate is placed below and above the wafer, and pressed together with clamps. This improves the wafer to mask distance and hence accuracy.

4. The glass plates and wafer are placed beneath an UV-light and exposed for several seconds. This exposure will cause the SU-8 to crosslink, making those areas solid and immune to the developer. If the photoresist is exposed for too long, the area of crosslinking will increase and structures will be wider as more material has cross-linked. If the photoresist is not exposed enough, the structures will end up smaller than intended and may even be washed away as the photoresist near the bottom does not crosslink. For the initial device the exposure time is 60 seconds.

5. The wafer is removed from between the glass plates and placed on the 65 °C hotplate. When the wafer is properly exposed to the UV-light, the structures will be visible after 10-15 seconds. After 3 minutes the temperature is raised to 95 °C, followed by a cooling down to room temperature. This step is called the hard bake and is used to strengthen the crosslinking induced by the UV-light.

6. The wafer is placed in a developer liquid (Mr-dev 600, Microresist Technology), which will remove any SU-8 that has not been exposed to the UV-light. The result is a wafer with the design structure of a specific height on top of it, which will be called the 'master' and is used as a mould to create the PDMS devices (next section). If the wafer remains in the developer liquid for too long, the cross-linked areas will also start to be removed and sections of the microstructure might start to float. This is called overdeveloping and an example is shown in figure C.1 . For the initial design, this development time was 20 minutes.

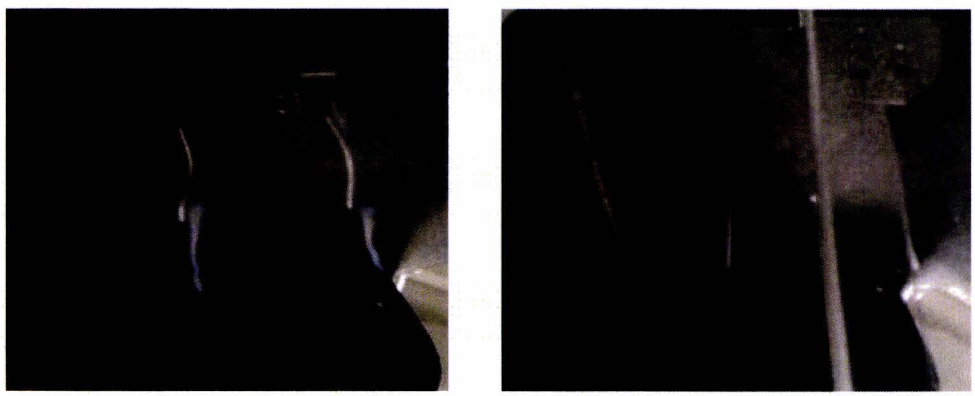

Figure C.1: Images of wafer made using soft lithography. The left image shows an overdeveloped wafer, who spend too much time in the developer fluid during the soft lithography process. The right image shows a successfully created wafer.

The parameter used in the steps above are for the creation of the initial device. They are shown in the table below, along with the parameters used for the creation of the final device.

Initial design	
Photoresist	SU-8 2050
Spincoater	500 RPM for 10 seconds
	1500 RPM for 30 seconds
Exposure time	60 seconds
Developer	Mr. dev 600
Development time	20 minutes
Final design	
Photoresist	SU-8 2010
Spincoater	300 RPM for 10 seconds
	600 RPM for 10 seconds
	900 RPM for 10 seconds
	1000 RPM for 20 seconds
Exposure time	40 seconds
Developer	Mr. dev 600
Development time	5 minutes

Appendix D

Using PDMS to fabricate a microfluidic device from the master wafer

To make microfluidic devices capable of handling liquids, PDMS (polydimethylsiloxane) is used, which is a polymeric silicone. When a curing agent is added to the PDMS, it will cause the polymers to crosslink, transforming the PDMS from a visco-elastic state to an elastic state. This allows it to replicate the microscale structures of the master. The master is placed in a petri dish and 65 grams of PDMS, mixed with 6,5 gram of curing agent, is added, followed by moving the petri dish to the oven. Here it is left to cure (crosslink) at 75 °C for 1.5 hours. The curing is slow at room temperature and it would take several days to acquire an elasticity high enough to mimic the master with enough accuracy, hence the increased temperature is applied to allow a faster procedure. Once the PDMS is cured, the device can be cut out using a razor blade, taking care not to damage the master. Holes are punched for the connection between the microchannels and the tubing using a biopsy punch (Harris unicore 1.20) as shown in figure D.1. To complete a device the surface of both the PDMS and a microscopy slide are treated with a corona discharger to activate the surfaces. All surfaces are treated for approximately 20-25 seconds. After the treatment, the surfaces are placed on top of each other, and bonded together. Placing the completed device in the oven for 15 minutes at 70 °C will enhance this bond even more.

Figure D.1: A biopsy punch

Appendix E

Experimental setups

E.1 Initial design

This setup consists of, as is also shown in figure E.1 , the following items :

- A syringe pump with display (Harvard Apparatus PHD 2000 infusion)
- 3 pieces of tubing with a length of approximately 15 cm (SCI micro medical tubing, I.D 0.86 mm x O.D 1.32 mm, Lake Havasu city, America)
- A small glass container for outlet output.
- 2 needles with blunt tip (Techcon, TE Series 20 AWG X .25" LG, Pink)
- 2 plastic syringes of 1 ml (HWS 1 ml Norm-ject, Luer tip)
- 1 set of plastic tweezers
- 1 sealing clip, a device capable of squeeze tubing preventing any liquid from moving through, as is shown in figure E.1 (WeLock PA 70)
- Agarose beads
- Purified water
- A microscope with up to 40x magnification (Carl Zeiss B.V. Axiovert 25)
- A camera USB CCD (Monochrome Camera,The Imaging Source, Bremen,Germany)

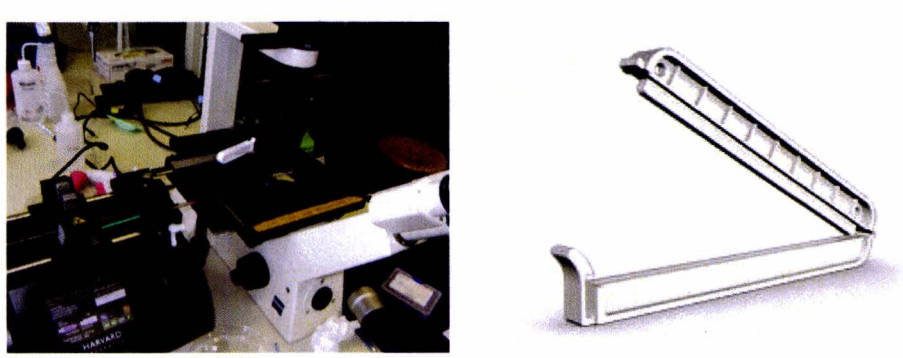

Figure E.1: The left image shows the experimental setup. To the left is the syringe pump, on which lies the syringe. A blunt needle connects the syringe to the tubing going into the device placed on the microscope. The right image shows a sealing clip, used to block tubing.

E.2 Final design

This setup consists of the following items :

- A syringe pump with display (Harvard Apparatus PHD 2000 infusion)
- 3 pieces of tubing with a length of approximately 15 cm (SCI micro medical tubing, I.D 0.86 mm x O.D 1.32 mm, Lake Havasu city, America)
- 2 needles with blunt tip (Techcon, TE Series 20 AWG X .25" LG, Pink)
- 2 plastic syringes of 1 ml (HWS 1 ml Norm-ject, Luer tip)
- 1 set of plastic tweezers
- 1 sealing clip, a device capable of squeeze tubing preventing any liquid from moving through, as is shown in figure 14B (WeLock PA 70)
- 3 metal connectors
- PBS
- BSA
- HL-60 cells and medium
- Ethanol (for cleaning afterwards)
- A microscope with up to 40x magnification (Carl Zeiss B.V. Axiovert 25)
- A camera USB CCD (Canon Powershot A720)

E.2.1 Metal connectors

During the first couple of experiments the tubing would not remain in the inlet for the entire experiment. When the flow rate was increased, the tubing would disconnect and the experiment had to be cancelled. For this reason a connector piece has been created to connect the tubing and the device. This connector is made from a needle with a blunt tip, of which the plastic cover has been removed, turning the needle into a simple hollow cylinder. The cylinder is then bent at a straight angle, after which the vertical part is placed in the inlet of the device, while the horizontal is connected to the tubing. The metal allows the connector to be placed much deeper in the PDMS inlet keeping it in place more easily.

E.2.2 PBS

Phosphate Buffered Saline (abbreviated PBS) is a buffer solution commonly used in biological research. It is a water-based salt solution containing sodium chloride, sodium phosphate, and, in some formulations, potassium chloride and potassium phosphate. The buffer's phosphate groups help to maintain a constant pH. The osmolarity and ion concentrations of the solution usually match those of the human body (isotonic). PBS is often used when handling cells because it is isotonic and non-toxic to cells. For the experiment the PBS is used as the operating fluid, replacing the purified water of the previous design. Before the experiments, the PBS is filtered to prevent debris and dust.

E.2.3 BSA

Bovine Serum Albumen (abbreviated BSA) is used to prevent the adhesion of the HL-60 cells to the PDMS. 2 wt.% is dissolved in PBS to create a solution, which can be flushed through the devices. The PDMS will absorb the BSA solution and prevent enzymes from adhering to it. After dissolving the BSA, the solution is filtered to prevent debris from BSA that did not dissolve.

E.2.4 Medium and culture

Medium is important for cell culturing as it contains all supplements necessary for the cell to reproduce. The HL60 cells were grown in RPMI 1640 medium supplemented with 10% fetal bovine serum (FBS), 1% L-glutamine and 1% Penicillin/Streptomycin.

Appendix F

Experimental procedure for the initial design

We start by dispersing the beads in the purified water a solution with approximately 10^6 beads/ml is created. A 1 ml syringe is filled with the solution and the blunt tip needle is put on the outlet of the syringe. A piece of tubing is connected to the tip and the syringe is compressed to fill the tubing with the solution. The other syringe is filled with purified water and treated identically. With help of the tweezers, the free end of the tubing with the solution is placed in the inlet without the filter (as the filter would enhance clogging behaviour by reducing the width of the channel, because of its function for filtering debris). As the diameter of the tubing is equal to the hole, the PDMS needs to elastically deform around the tubing, making it hard to insert the tubing but ensuring it remains in place by friction. The tubing with the purified water is placed in the inlet with the filter. The third piece of tubing is placed in the outlet and the small glass container is placed beneath its exit to drain the used fluids.

The experiment starts by blocking the tubing with the solution with the sealing clip and placing the syringe with the purified water in the syringe pump. The purified water is pumped into the microfluidic device at 10 μL/min and left for 5 minutes to fill the entire device with purified water. Air remaining in the device will slowly diffuse through the PDMS because of the pressure induced by the syringe pump. After these 5 minutes of pumping the syringe pump is stopped and the syringe gets replaced with the syringe containing the solution with beads. The solution is now flown through the device at 20 μL/min and the beads are tracked through the bypass channels until they finally get trapped.

Appendix G

Experimental procedure for the final design

G.1 Coating

3 devices are prepared for each experiment, in case some of them have flaws. First the devices need to be coated to prevent cells from adhering to the wall of the device. A syringe is filled with the 2% BSA solution and a needle with a blunt tip is placed on top of the syringe. The tip is then placed at the outlet of the device, and gently pressed. By observing the device under the microscope the fluid can be seen to travel up to the two inlets. Every time a needle is switched (for example from the cell solution to the PBS) it will cause some PDMS debris, which may clog the device. At the length scales of the initial devices, this did not pose a problem, as most of the debris is around 5-8 μm in size which could not easily clog a 60 μm channel. With the current design, the debris started to clog the device when flushing at a speed of 0.5 μL/min. The debris came mostly from switching connectors in and out of the device. Therefore the outlet was used to coat, working around the need to put a connector into an inlet and henceforth reduce the amount of PDMS debris. After applying the coating, the devices were put in a petri dish for 1.5 hours to allow the PDMS to absorb the BSA solution. sdfgsd

G.2 Experimental steps

The experimental steps are as follows

1. A syringe, with tubing connected, is filled with PBS. A connector is placed at the end of the tubing and the connecter is placed in the outlet of the device. The device itself is placed on the moving stage and remains there for the rest of the experiment. The syringe is attached to the syringe pump and the BSA solution that was applied 1.5 hours earlier is flushed from the system at a speed of 5 μL/min. The BSA solution, if left in the device for too long, will dry and the BSA will solidify, causing debris which hinders cell transport. The flushing through the outlet also cleans any debris that may have been stuck in the inlets. If debris was at the outlet, because of the placing of the connector, it would either be flushed all the way to the inlet, or got stuck at the bottleneck below the last trapping area, where it can be flushed out by applying a flow from the inlet later on.
2. The other two pieces of tubing are each attached to a connecter, and one of them is placed in the outlet after removing the connector with the PBS tubing, the other one is placed in an inlet. The connector with the PBS tubing is placed in the other inlet and the sealing clip is used on the tubing of the outlet tubing, in order to create a flow between the two inlets. These are now flushed at a speed of 0.5 μL/min as the placing of the connectors has detached debris from the inlets which must be cleaned.
3. The sealing clip is removed from the outlet tubing as well the connector with the empty tubing. The other syringe, without any tubing, is filled with a cell solution from the culture. This solution has been modified to have a cell concentration of approximately 10^6 cells/ml. The blunt tip needle is then placed in the unused inlet and is gently pressed to create a pressure allowing the cell solution to enter the device.

4. When cells can be seen flowing through the device, the syringe with the cell solution is removed and 5 min is waited to allow the pressure to stabilize, reducing the speed of the cells and the pressure drop over the bypass channels, allowing cells to get trapped and not squeeze through instantly. The connector with the tubing used for step two is placed back in the now unused inlet and the tubing is blocked using the sealing clip. This ensures all flow from the PBS tubing will go to the outlet.

5. The PBS is flown through the device at 0.5 μL/min. At this flow rate, cells get trapped but are not pushed through the trap. When no more cells are flowing through the bypass channels, which can take up to 5 minutes, the camera is placed on the microscope and a movie is made, using a zoom of 40x, starting from the first trapping area down to the last one. The stage attached to the microscope is used to move the microscope focus in a straight line. If a cell is detected in a trap, the camera maintains its position for 1 second to get some frames with a higher focus, which can be analysed later. When all trapping areas have been filmed, the flow rate is increased by 0.5 μL/min and we wait for 2 minutes for the flow to stabilize. After this stabilization period the trapping areas are filmed once again and step five is repeated until all cells have squeezed through their traps.